Electronic Supplementary Material (ESI) for Journal of Materials Chemistry A.

Organometallic precursor induced defects-enriched mesoporous CeO_2 with high specific surface area: preparation and catalytic performance

Shaowei Yang, [a] Haidong Shen, [a] Fang Cheng, [a] Chen Wu, [a] Yueling Cao, [a] Sifei Zhuo, [a]
Qiuyu Zhang* [a], Hepeng Zhang, *[a]

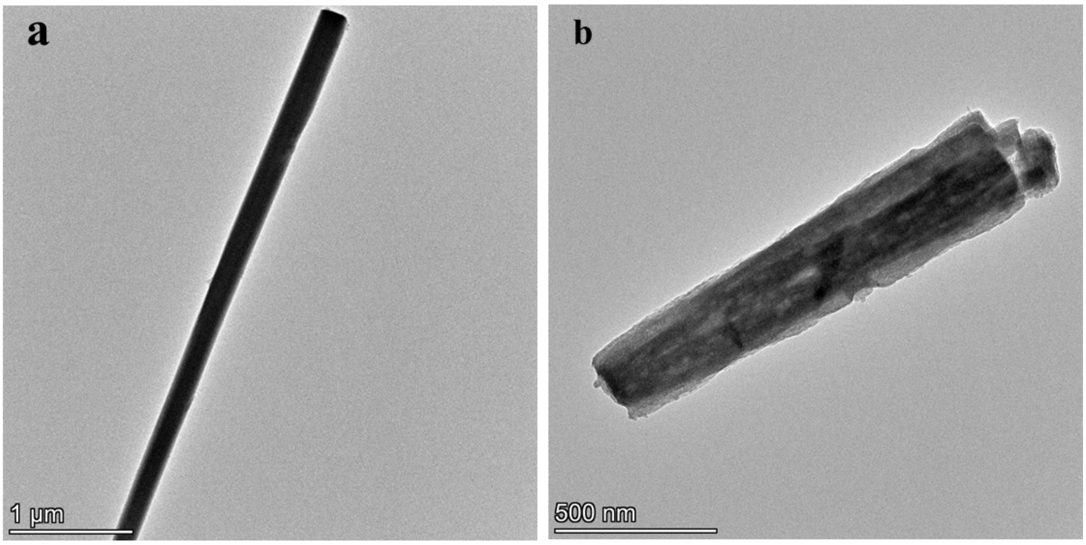

Figure. S1 (a) the TEM of precursor synthesized by cerium nitrate hexahydrate; (b) the TEM of P_{fa}-7.

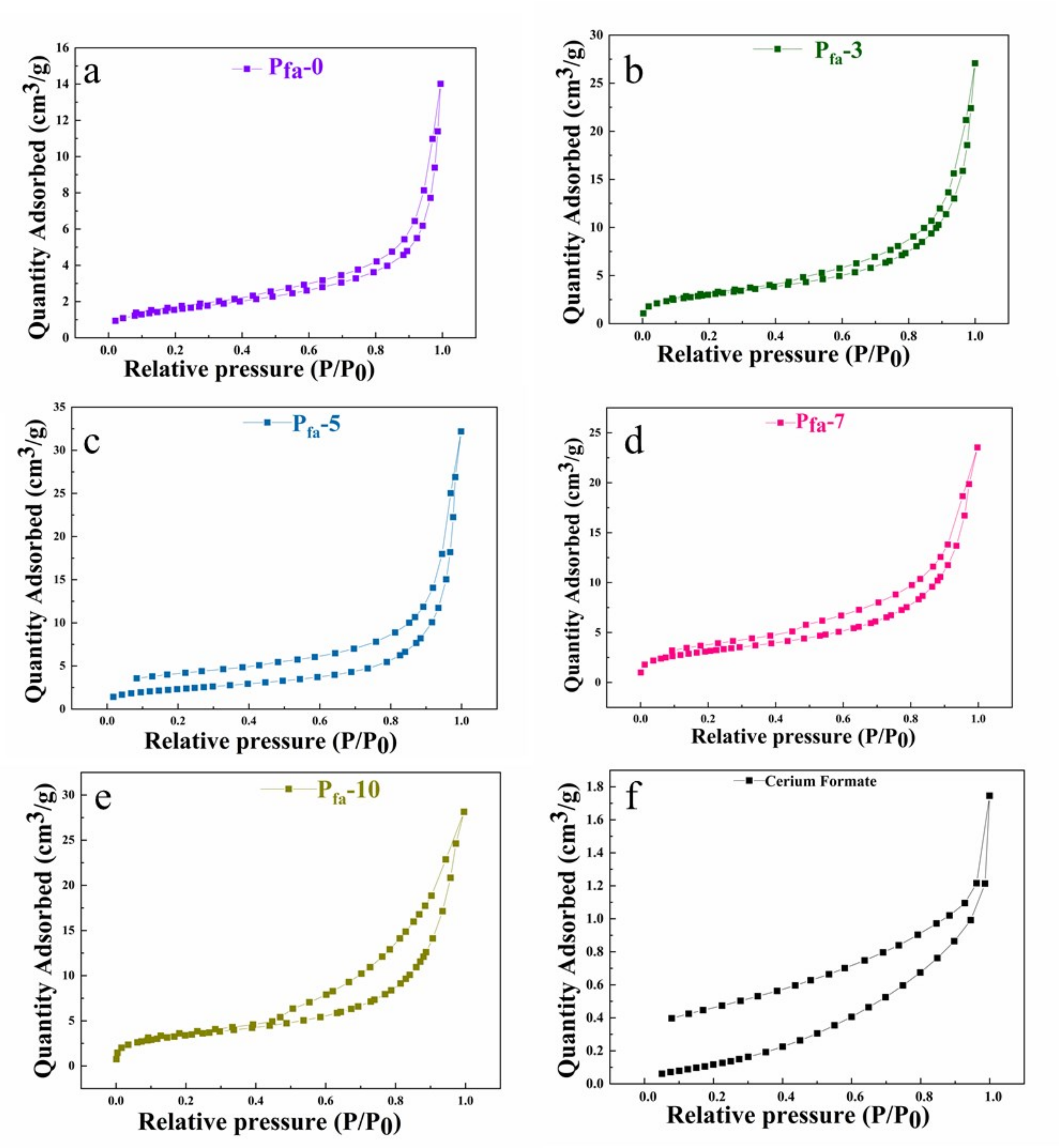

Figure S2 (a-f) Nitrogen adsorption−desorption isotherms of the six different kinds precursors.

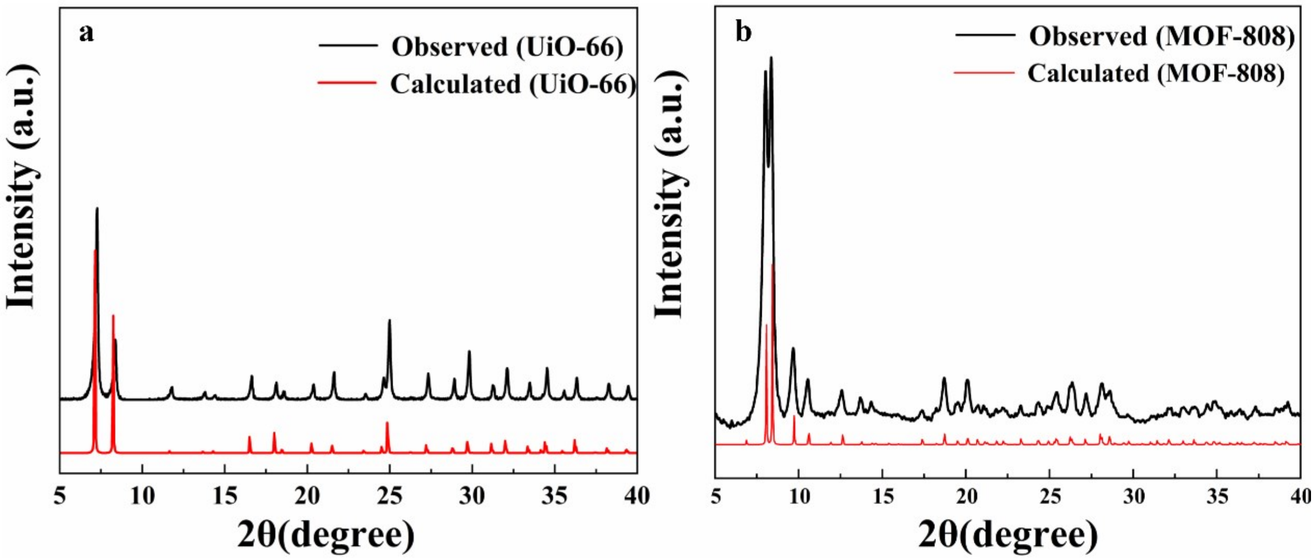

Figure S3. (a) XRD patterns of the UiO-66; (b) XRD patterns of the MOF-808.

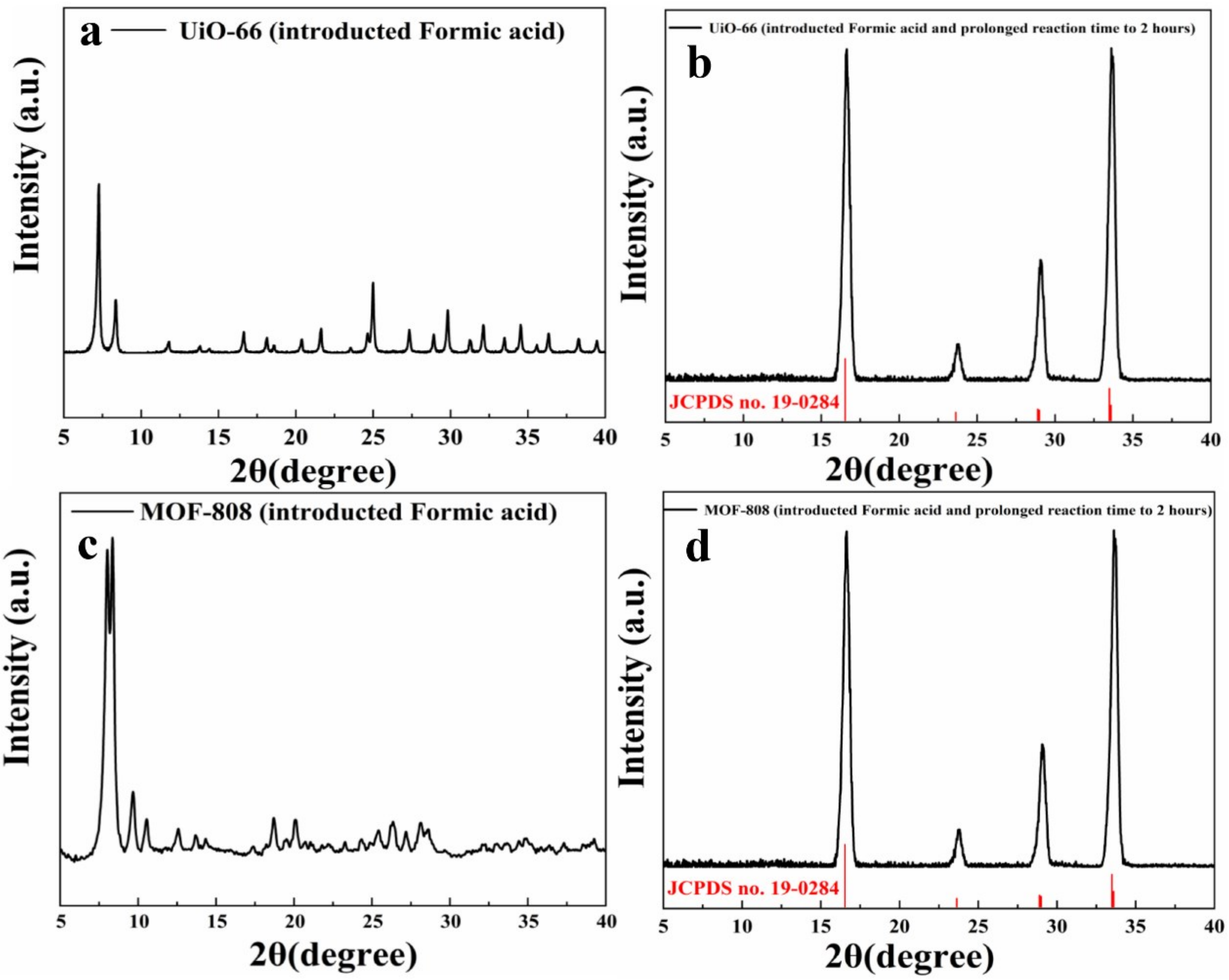

Figure S4. XRD patterns of (a) UiO-66 (introduced Formic acid), (b) UiO-66 (introduced Formic acid) that prolonging reaction time to 2 hours, (c) MOF-808 (introduced Formic acid) and (d) MOF-808 (introduced Formic acid) that prolonging reaction time to 2 hours.

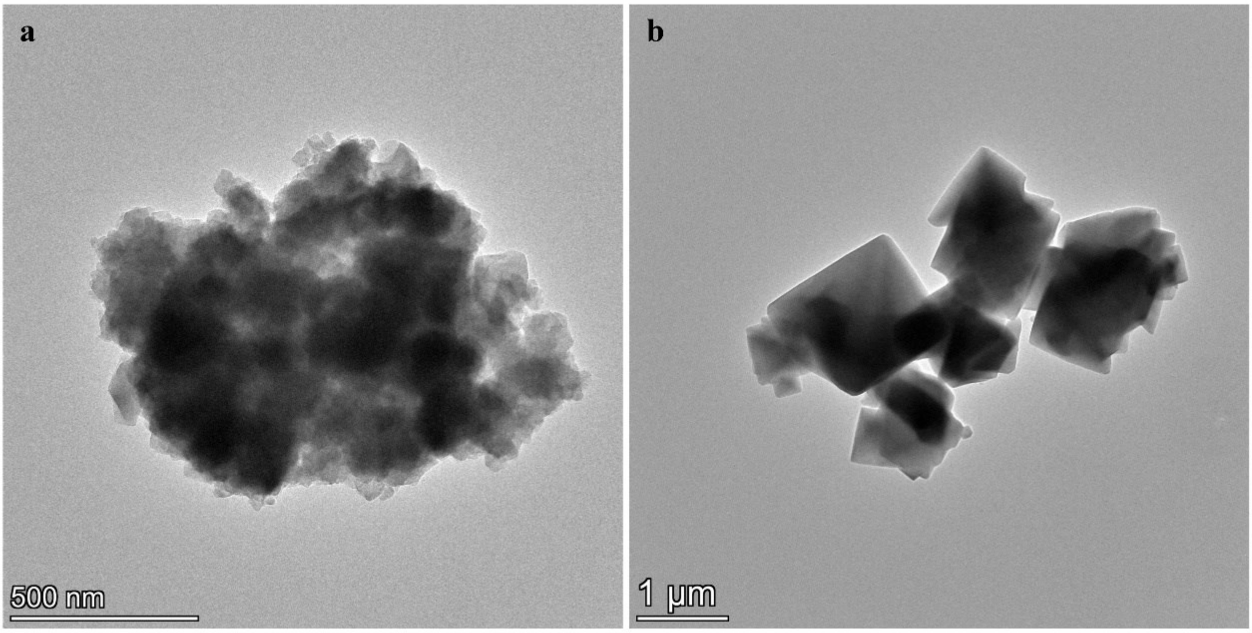

Figure S5. (a)TEM image of MOF-808; (b) TEM image of UiO-66.

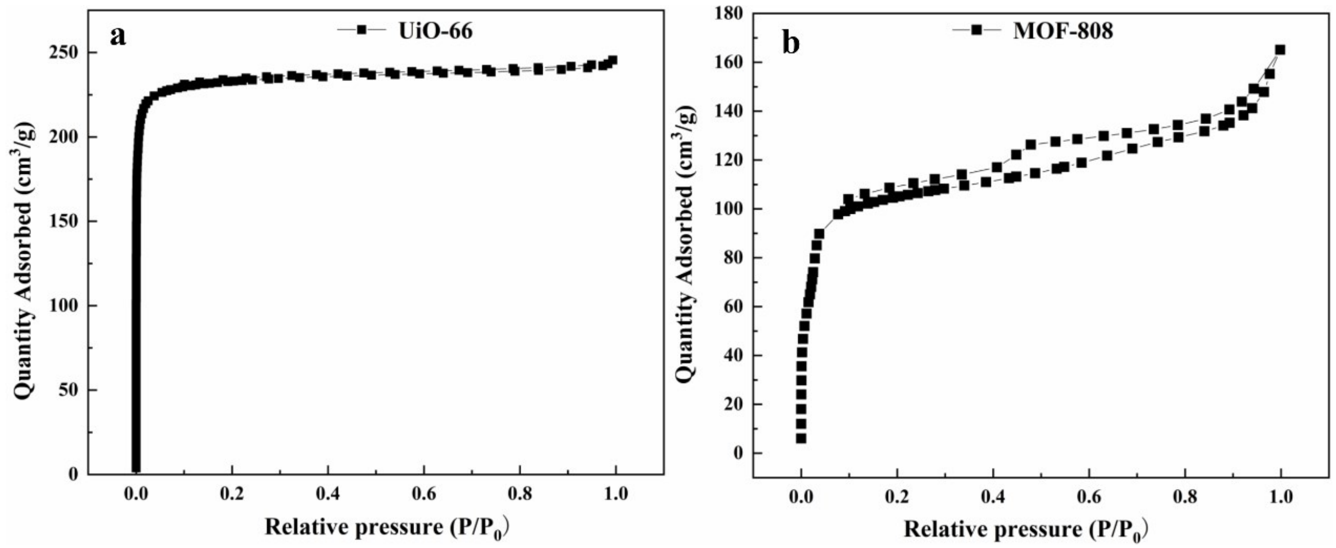

Figure S6. (a) Nitrogen adsorption−desorption isotherms of the UiO-66; (b) Nitrogen adsorption−desorption isotherms of the MOF-808.

To explore the properties of electronic cloud density of carboxylic oxygen atoms and steric hindrance, some calculations were performed. Based on density functional theory (DFT), with B3LYP as the calculation method, 6-31G as the base group, and Gaussian 03W as the calculation software, the configurations of the reactants, products and transition states were optimized in turn, and the corresponding enthalpies and Gibbs free energies were obtained.

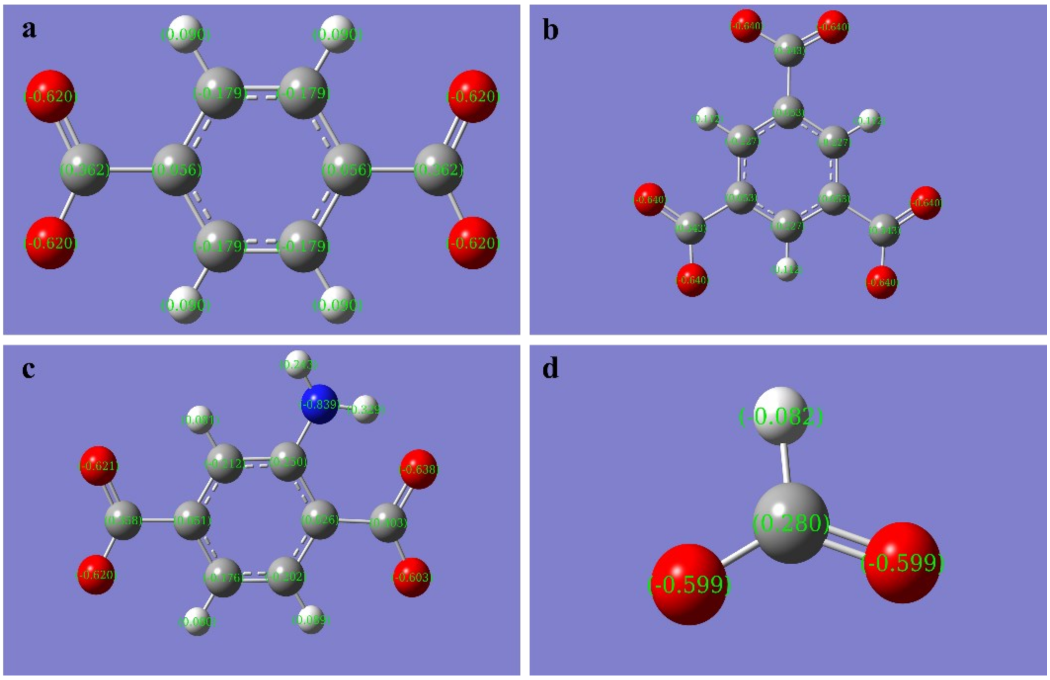

Figure S7. DFT calculation of (a) 1,4-benzenedicarboxylic acid (H_2BDC), (b) Benzene-1,3,5-tricarboxylic acid (H_3BTC), (c) 2-Aminoterephthalic acid (NH_2H_2BDC) and (d) formic acid (HCOOH).

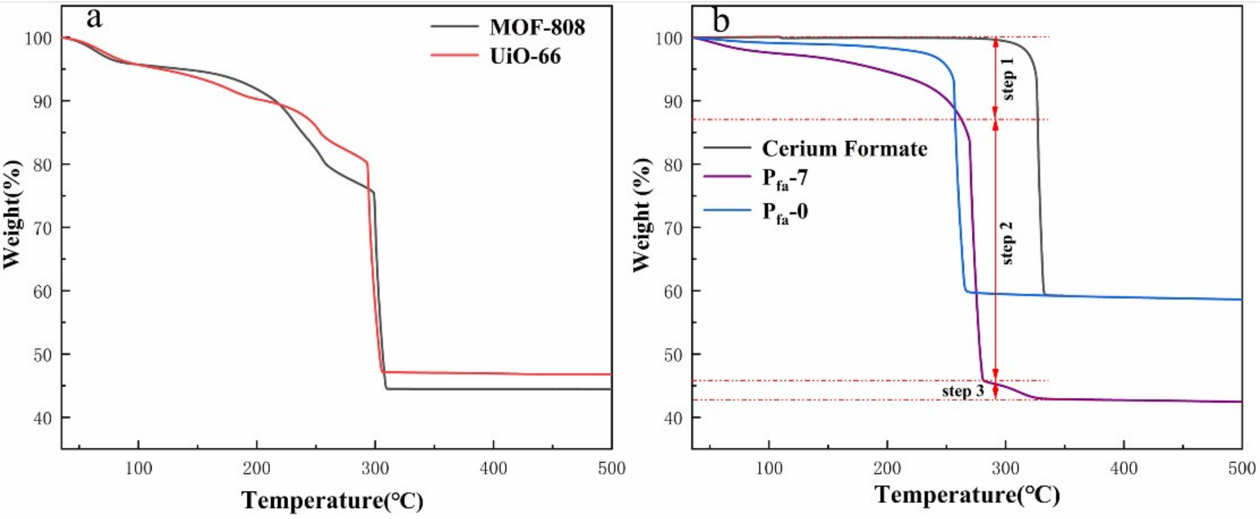

Figure S8. (a) TGA curves of the precursors of MOF-808 and UiO-66; (b) TGA curves of the precursors ofcerium formate, P_{fa}-7 and P_{fa}-0.

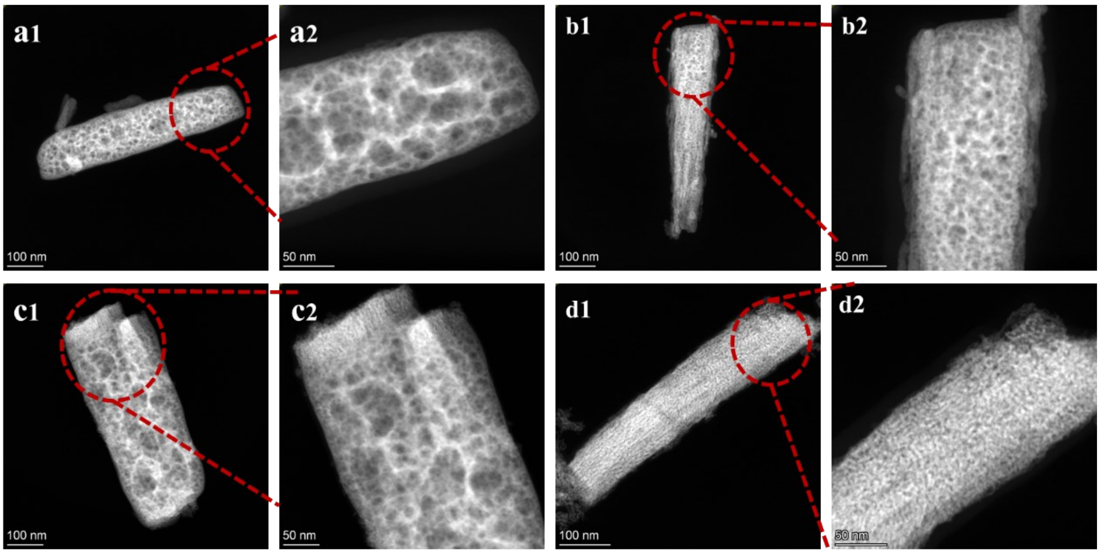

Figure S9 (a1 and a2) the STEM of P_{fa}-7 after pyrolyzed at 220 ^{o}C; (b1 and b2) the STEM of P_{fa}-7 after pyrolyzed at 240 ^{o}C; (c1 and c2) the STEM of P_{fa}-7 after pyrolyzed at 260 ^{o}C; (d1 and d2) the STEM of P_{fa}-7 after pyrolyzed at 280 ^{o}C.

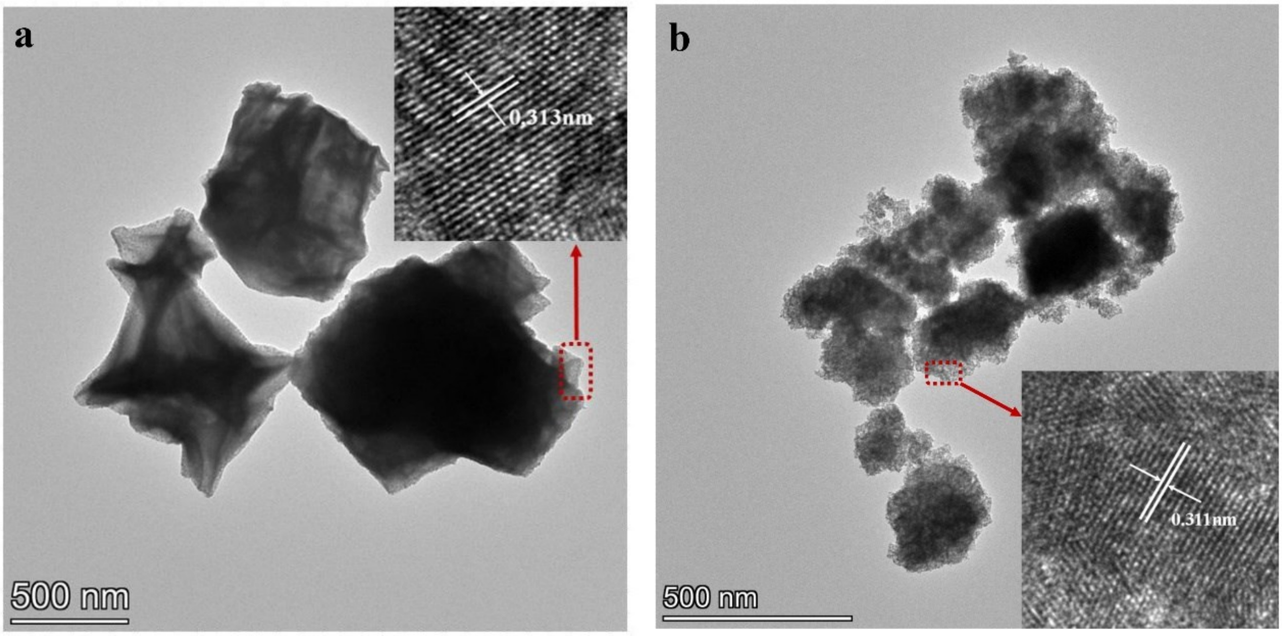

Figure S10. (a) TEM and HRTEM image of CeO_2-UiO-66; (b) TEM and HRTEM image of CeO_2-MOF-808.

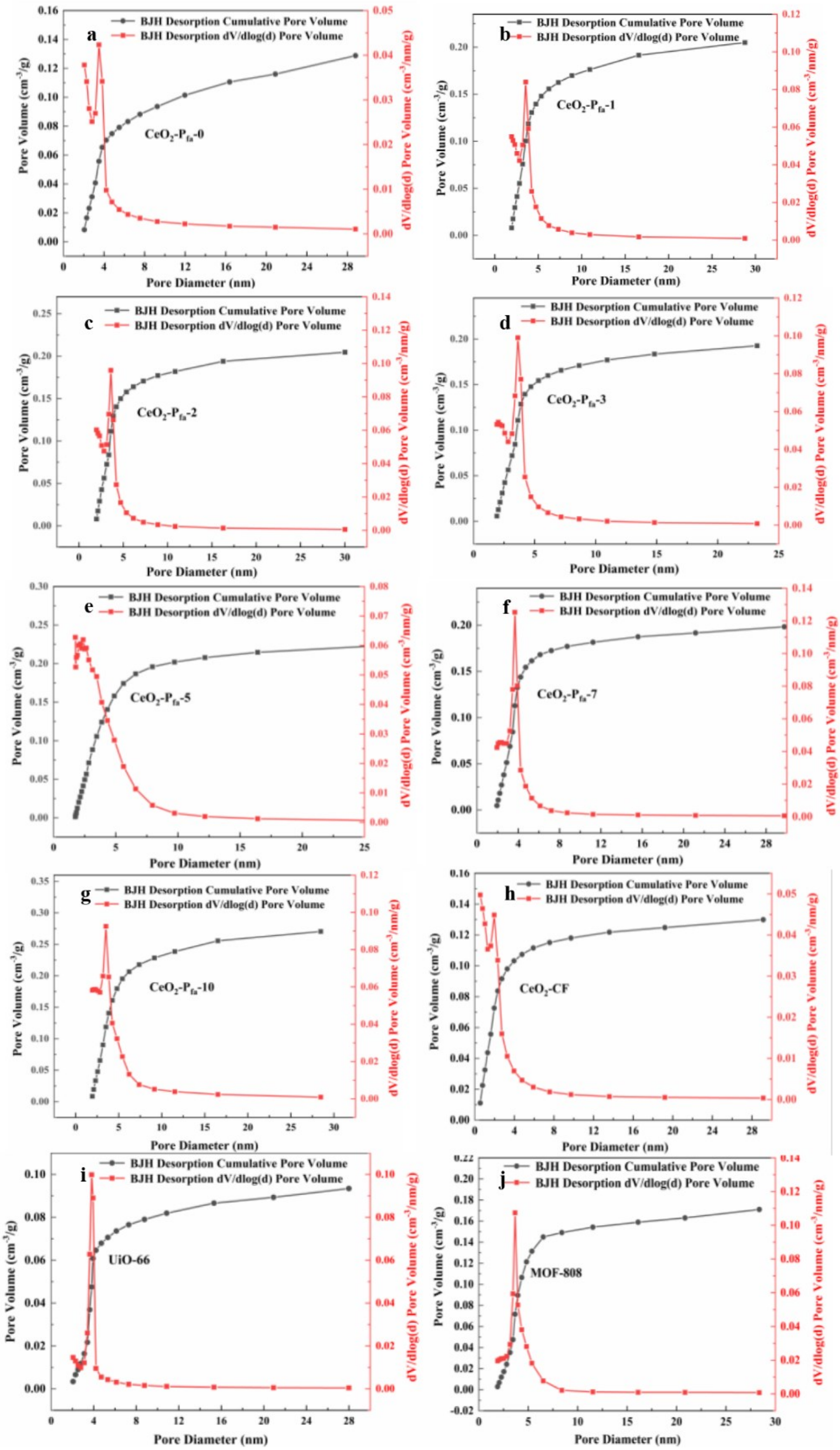

Figure S11. BJH Desorption Cumulative Pore Volume curves of different kinds of CeO$_2$.

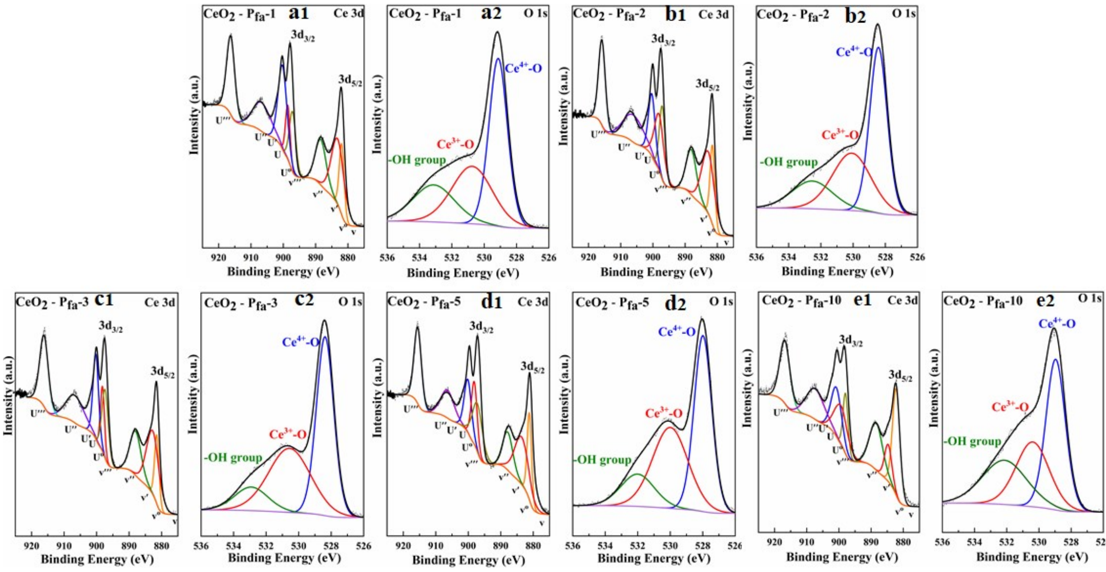

Figure S12. (a1, b1, c1, d1 and e1) XPS spectra of the Ce 3d; (a2, b2, c2, d2 and e2) XPS spectra of the O 1s that are prepared from decomposition of precursor including P_{fa}-1, P_{fa}-2, P_{fa}-3, P_{fa}-5 and P_{fa}-10.

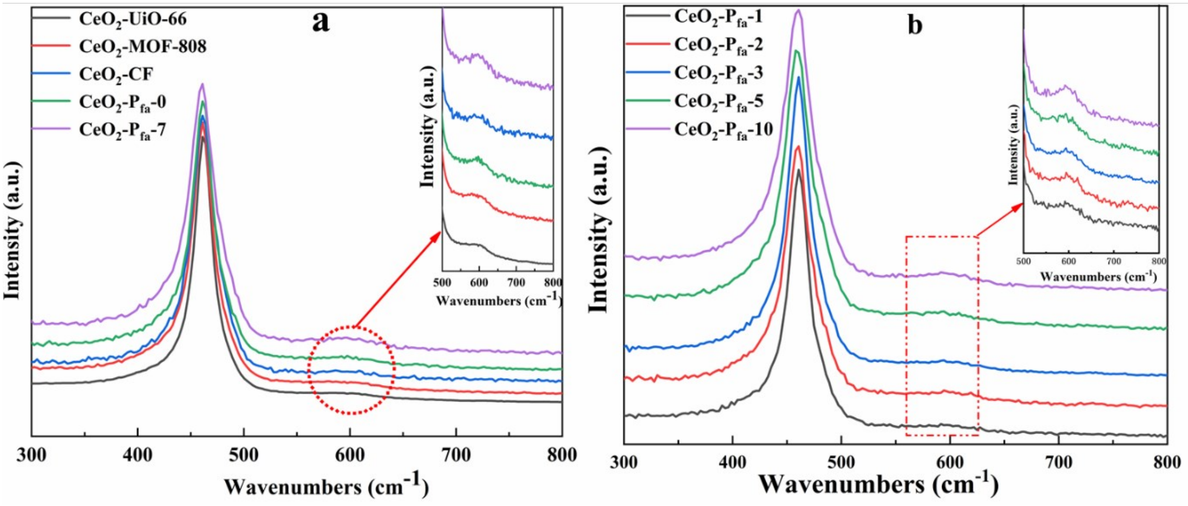

Figure S13. (a) Raman spectra analysis of the different kinds CeO_2 including CeO_2-UiO-66, CeO_2-MOF-808, CeO_2-CF, CeO_2-P_{fa}-0, and CeO_2-P_{fa}-7; (b) Raman spectra analysis of the different kinds CeO_2 including CeO_2-P_{fa}-1, CeO_2-P_{fa}-2, CeO_2-P_{fa}-3, CeO_2-P_{fa}-5 and CeO_2-P_{fa}-10.

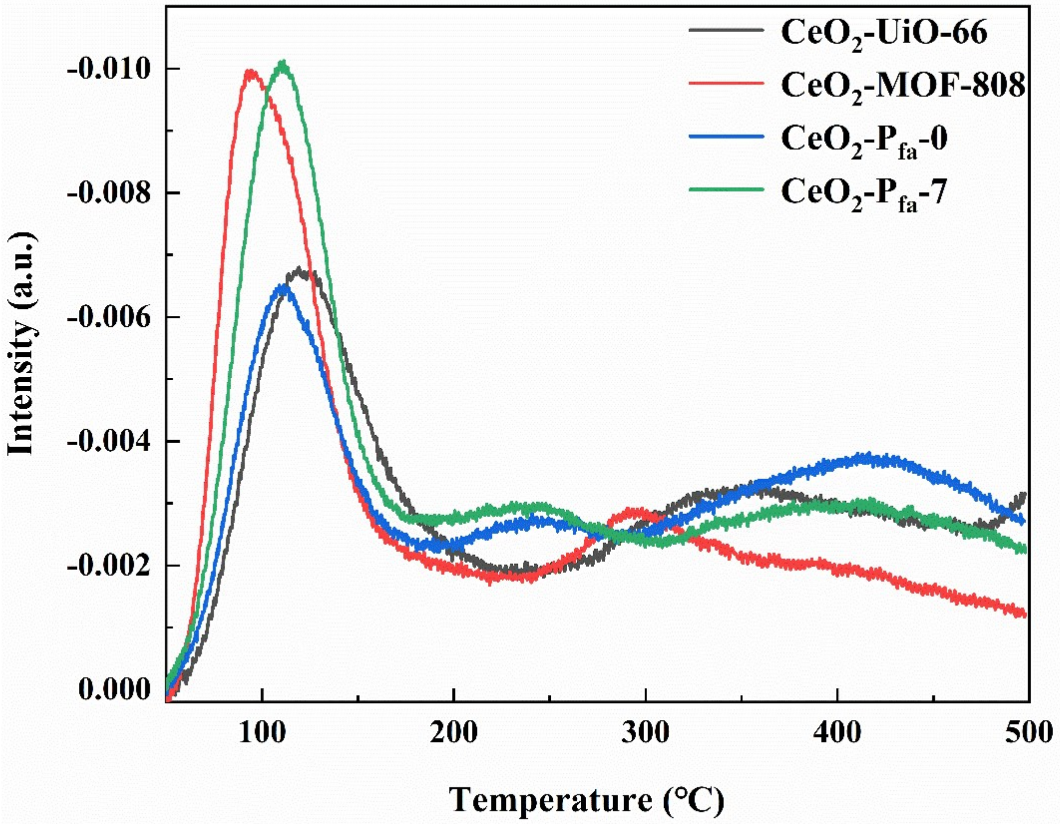

Figure S14. CO_2-TPD profiles of the P_{fa}-7, P_{fa}-0, MOF-808 and UiO-66.

Table S1 Comparison of conversion and selectivity on the reaction of benzyl alcohol and aniline

Catalysts	Reactive conditions	Conversion of benzyl alcohol (%)	Selectivity (%)	Refer
CeO_2-P_{fa}-7[a]	333 K, 4, air	69.1	82.4	This article
CeO_2-P_{fa}-7[a]	333 K, 6h, air	81.0	88.7	This article
CeO_2-P_{fa}-7[a]	333 K, 8 h, air	92.9	>99.0	This article
CeO_2-5 [a]	333 K, 8 h, air	72.0	97.0	[1]
CeO_2-5 [a]	333 K, 24 h, air	≥99.0	≥99.0	[1]
CeO_2 [b]	333 K, 24 h, air	96.0	97.0	[2]
CeO_2 rod [c]	333 K, 12 h, 1 atm of O_2	99.0	94.0	[3]
CeO_2-100 [d]	333 K, 9h, air	31.0	96.0	[4]
hollow CeO_2 [e]	333 K, 6 h, air	55.0	97.0	[5]
hollow CeO_2 [e]	333 K, 12 h, air	99.0	98.0	[5]

[a] Reaction conditions: Catalyst CeO_2 (50 mg), Benzyl alcohol (1.0 mmol), aniline (2.0 mmol), meta-xylene (1.6 mL), air; [b] Conditions: Benzyl alcohol (1.0 mmol), aniline (2.0 mmol), mesitylene (1.5 g), CeO_2 (50 mg), air; [c] Conditions: Benzyl alcohol (0.5 mmol), aniline (0.6 mmol), p-xylene (2 mL), CeO_2 (100 mg), O_2; [d] Conditions: benzyl alcohol (1 mmol), aniline (1 mmol), 50 mg catalyst, solvent (3 mL), air; [e] Reaction conditions: Catalyst CeO_2, (20 mg), Benzyl alcohol (1.0 mmol), aniline (2.0 mmol), and mesitylene (1.5 mL) air. Hollow CeO_2 synthesized by hard template method.

Table S2 Catalytic abilities and physical properties of different kinds of ceria

Catalyst	Conversion (%)	Selectivity (%)	Ce^{3+} (%)[a]	Ce^{3+}-O (%)a
CeO2-Pfa-0[b]	40.9	69.8	21.5	21.2
CeO2-Pfa-3[b]	55.7	73.8	29.6	39.0
CeO2-Pfa-5[b]	60.2	70.1	32.3	40.9
CeO2-Pfa-7[b]	62.7	80.7	36.7	53.4
CeO2-Pfa-10[b]	54.6	78.3	23.4	30.6
CeO2-CF [b]	30.5	57.0	23.6	18.7
CeO2-UiO-66 [b]	30.0	36.3	20.4	29.5
CeO2-MOF-808 [b]	47.8	62.8	27.2	32.2

[a] The proportion of Ce^{3+} and Ce^{3+}-O were calculated by the result of XPS analysis based on formula of $Ce^{3+}/(Ce^{3+} + Ce^{4+})$ and Ce^{3+}-O/ [(Ce^{3+}-O) + (Ce^{4+}-O) + (-OH group)];

[b] Reaction condition: benzyl alcohol 1.0 mmol, aniline 2.0 mmol, ceria 25 mg, 1000 rpm, 60°C, 8 h, air.

Table S3 The result of the conversion per unit S_{BET} of all samples

Catalyst	Conversion (%)	S_{BET} (m^2/g)	Conversion per unit S_{BET}
CeO_2-P_{fa}-0	62.3	132.3	9.4
CeO_2-P_{fa}-1	68.3	180.3	7.6
CeO_2-P_{fa}-2	74.7	181.5	8.2
CeO_2-P_{fa}-3	76.7	183.8	8.4
CeO_2-P_{fa}-5	89.9	204.6	8.8
CeO_2-P_{fa}-6	91.6	191.27	9.6
CeO_2-P_{fa}-7	92.9	171.9	10.8
CeO_2-P_{fa}-10	82.4	203.1	8.2
CeO_2-CF	59.6	137.3	8.6
CeO_2-UiO-66	49.3	79.7	12.4
CeO_2-MOF-808	70.5	119.3	11.8

References

1. H. Zhang, C. Wu, W. Wang, J. Bu, F. Zhou, B. Zhang and Q. Zhang, *Applied Catalysis B Environmental*, 2018, **227**, 209-217..
2. M. Tamura and K. Tomishige, *Angewandte Chemie International Edition*, 2015, **54**, 864-867.
3. Zhixin. Zhang, Yehong. Wang. Min, Wang. Jianmin. Lü, Lihua. Li, Zhe. Zhang, Mingrun. Li, Jingyang. Jiang and Feng. Wang, *Chinese Journal of Catalysis*, 2015, **36**, 1623–1630.
4. J. Qin, Y. Long, W. Wu, W. Zhang, Z. Gao and J. Ma, *Journal of Catalysis*, 2019, **371**, 161-174.
5. Yu. Long, Hongbo. Zhang, Zekun. Gao, Jiaheng. Qin, Yiting. Pan, Jinping. Zhao, Yuton.g Luo, Zhiping. Ma, Yucong. Xiong and Jiantai. Ma, *Inorganic Chemistry Frontiers*, 2019, **6**, 829-836.